

Pulsed Electron-Beam Irradiation Followed by Nitriding of Ti-6Al-4V Titanium Alloy¹

A.B. Markov, R. Günzel*, H. Reuther**, N. Shevchenko**, Yu.Kh. Akhmadeev, P.M. Schanin, N.N.Koval, V.P. Rotshtein, D.I. Proskurovsky

*Institute of High-Current Electronics, 2/3 Akademicheskii pr., Tomsk, 634055, Russia,
Tel (3822)491695, Fax (3822)491695, E-mail almar@fromru.com*

** APT GmbH, Bautzner Landstr. 45, Großerkmannsdorf, 01454, Germany*

*** Forschungszentrum Rossendorf e. V., Institute of Ion Beam Physics and Materials Research, P.O.B. 51 01 19, Dresden, 01314, Germany*

Abstract – Pre-irradiation of Ti-6Al-4V titanium alloy with a low-energy, high-current electron beam of microsecond duration allowing surface melting was shown is an efficient way for enhancement the following plasma nitriding. Materials investigation revealed the larger fraction of TiN and Ti₂N phases as well as the concentration of nitrogen in the surface layer for the pre-irradiated sample than those for the non-irradiated one. This combined electron beam irradiation followed by plasma nitriding treatment appears to be a promising tool for the surface modification of titanium alloys.

1. Introduction

It is well known that titanium alloys have some attractive properties enabling them to be used in many industries such as aerospace, marine, and medicine, while their poor tribological properties often are an obstacle in mechanical engineering applications [1]. The latter properties can be improved by applying various surface treatments, for instance, nitriding, ion implantation, electron-beam, and ion-beam irradiation. One of the most appealing of them is a nitriding allowing occurrence on the sample surface the TiN phase desirable due to its high wear resistance properties. Conventionally nitriding is conducted at high temperatures. The higher is the surface temperature of a sample the more efficient is the process of titanium nitriding and consequently the TiN phase formation. However the surface temperature during nitriding appeared to play a key role for the future properties of a processing material and in some cases can not be increased up to high values. The matter is, that a high-temperature plasma nitriding reduces the fatigue strength of titanium alloys. That is why over the last years techniques allowing nitriding at relatively low temperatures have been developed. One of them referred to as intensified plasma-assisted processing (IPAP) enables surface treatment at a relatively low temperature of 673–773 K [2].

Another reasonable way, excepting a modification of the nitriding process, of enhancement of titanium alloy nitriding at low-temperatures is a change of titanium alloy properties in the thin surface layer before nitriding. The latter maybe realized for instance with an irradiation by a low-energy, high-current electron beam (LEHCEB) of microsecond duration. It has been established earlier that martensitic phases referred to as α' and α'' occurred in the thin surface layer of (Ti-6Al-4V) alloy as a result of LEHCEB irradiation [3]. Moreover, it was revealed the grain refinement takes place in the surface layer of irradiated sample, resulting in existence of high-value residual stresses as well. All these factors may appear to be beneficial from the point of view of saturation of titanium alloy with nitrogen.

Aim of the research was to investigate the effect of electron-beam pre-irradiation on the process of titanium alloy (Ti-6Al-4V) low-temperature nitriding.

For this, two series of the titanium alloy specimens were used. One of them was pre-irradiated by e-beam and then both series were subjected to plasma cleaning by Ar and nitriding in Ar+N environment. The detailed experimental procedure and the results obtained are described below.

2. Experimental

Samples were disks 4 mm thick and 18 mm in diameter. They were cut from the same rod ingot of commercial Ti-6Al-4V alloy and subjected to a conventional mechanical polishing up to a surface roughness of 0.04 μm .

One series of the samples was irradiated by a LEHCEB in Ar plasma environment at a pressure of 0.03 Pa. The electron-beam parameters were: 2.5–3.5 μs pulse duration, 30 keV maximum electron energy, 2.5 J/cm² beam energy density, and 0.1 Hz pulse repetition rate. Number of irradiation

¹ The work was supported by WTZ Project No RUS 02/002

pulses was equal to 40. This electron beam allowed surface melting of the sample being irradiated. The detailed description of electron-beam source arrangement and fundamentals of electron beam generation and operation are presented elsewhere [4].

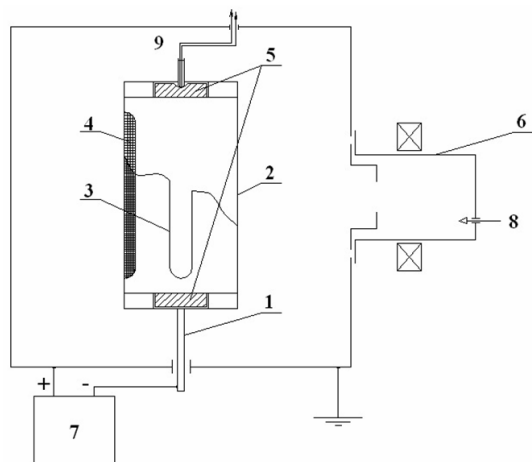


Fig. 1. The schematic diagram of nitriding installation: (1) holder, (2) hollow cathode, (3, 4) windows, (5) samples, (6) plasma source, (7) power supply of voltage bias, (8) gas input, (9) thermocouple

Further two series of the samples, namely, irradiated and non-irradiated were subjected to a sputtered cleaning with Ar ions and nitriding in Ar+N plasma environment at a pressure of 1 Pa and a specimen temperature of 773 K. Nitriding was conducted in the hollow-cathode glow discharge as shown in Fig. 1 and described in details elsewhere [5]. The plasma was generated in a plasma source (6) and then supplied into the vacuum chamber. Samples (5) were placed into hollow cathode (2) with the windows (3, 4). A voltage bias (0.75–1 kV) was applied between the cathode and the wall of vacuum chamber. In such a way both positive charged ions and neutral atoms of argon and nitrogen bombarded the inner surface of the hollow cathode including the surfaces of the samples.

Step-by-step processing procedure is shown in Tab. 1 in more detail.

Table 1. Step-by-step processing procedure

Processing	Number of shots/ processing time	T, K	P, Pa
1. E-beam pre-irradiation	40/–	300	0.03
2. Plasma cleaning (Ar)	–/10 min	370	0.5
3. Plasma nitriding (40 %Ar+60 %N)	–/250 min	773	1
4. Cooling	–/60 min		

Different test techniques such as scanning electron microscopy (SEM), X-ray diffraction (XRD) analysis, and Auger electron spectroscopy (AES) were applied for investigation of the processed materials.

XRD analysis in Bragg-Brentano and grazing incident geometry were carried out in a Siemens diffractometer D8 and D5000, respectively with mo-

nochromated CuK_α radiation. All XRD patterns were obtained with the scan step $2\Delta\theta=0.1^\circ$ and counting time equals to 30 s.

AES conducted using a Microlab 310 F system (FISONS) including sputter etching with 3 keV Ar ion beam of 1–2 A/mm^2 current density which hit the surface at an incidence angle of 42° .

3. Results and discussion

A. Temperature calculation

To analyze the experimental results one should clearly realize the difference between irradiated and non-irradiated sample. It is well known that pre-irradiation with an electron beam leads to the heating and melting of a thin surface layer. Consequent high-rate cooling of the layer allows the occurrence of new phases and changes the material morphology. Data of the most practical interest is the thicknesses of the melted layer and the heat-affected zone (HAZ). The former is a region where the most critical changes in material properties takes place and the latter one is a layer where any modification has been seen. To calculate these thicknesses it is necessary to solve a heating problem which in this case reduces to a numerical solution of the one-dimensional heat equation as it was described elsewhere [6].

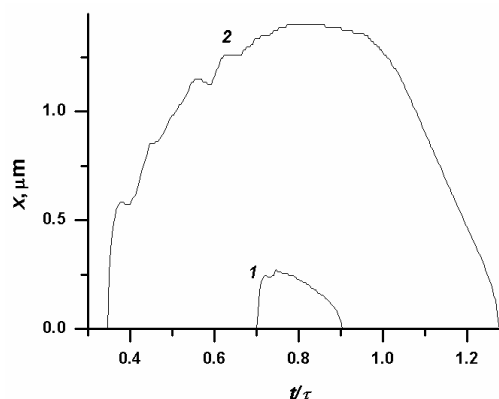


Fig. 2. Melting thickness vs time for Ti-6Al-4V alloy irradiated at 2.5 (1) and 3.25 (2) J/cm^2 , respectively. Here τ is pulse duration

In Fig. 2 the calculated state diagram of Ti-6Al-4V alloy target when being irradiated is presented. Each point of a curve is the position of the melt-solid boundary at a certain point of time. So the space below a curve accords to a melt-state and that above one accords to a solid-state. The irradiation was carried out at an average energy density of $E_s=2.5 \text{ J/cm}^2$ (curve 1). Nevertheless, one should take into consideration that in a case of multishot irradiation there is a dispersion in energy density from one shot to another and thereby a maximum energy density in a series of pulses will be larger than its average value. In our case, a maximum energy density is appeared to be 3.25 J/cm^2 (curve 2) which is 1.3 times that of the average value. As it can be seen from Fig. 1 for an

electron beam with an energy density of 3.25 J/cm^2 the maximum thickness of the melted layer equals to about $1.5 \text{ }\mu\text{m}$. It is in this region that grain refinement and hardening of material from the melt take place.

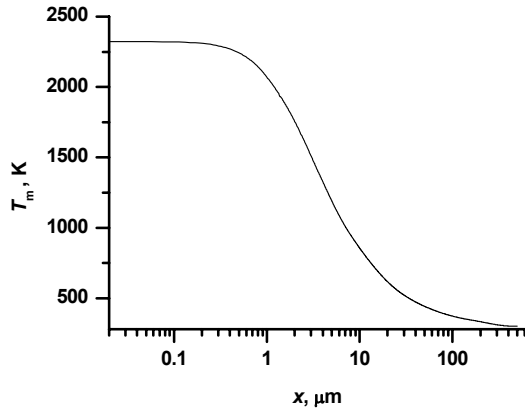


Fig. 3. Maximum temperature reached vs depth for Ti-6Al-4V alloy irradiated at 3.25 J/cm^2

From the predicted temperature-depth dependence shown in Fig. 3 a thicknesses of HAZ was estimated which appeared to be 30 microns. The temperature increment of material underneath HAZ was less than 200 K and thereby such a heating doesn't lead to phase transformation or critical change of the material morphology.

B. XRD and SEM investigations of irradiated sample

As it was revealed earlier and reported elsewhere [3] the irradiation of titanium alloy Ti-6Al-4V belonging to $\alpha+\beta$ type leads to the phase transitions and occurrence in the thin surface layer of specimen the martensitic α' and α'' phases. As it follows from the calculations the phase transition takes place in the thin surface layer of a thickness of 5–6 microns.

Fig. 4 provides a SEM image of the multishot irradiated surface. It confirms the data of XRD analysis revealing the existence of martensitic α' phase which is seeing inside the grains as parallel needle-like crystals.

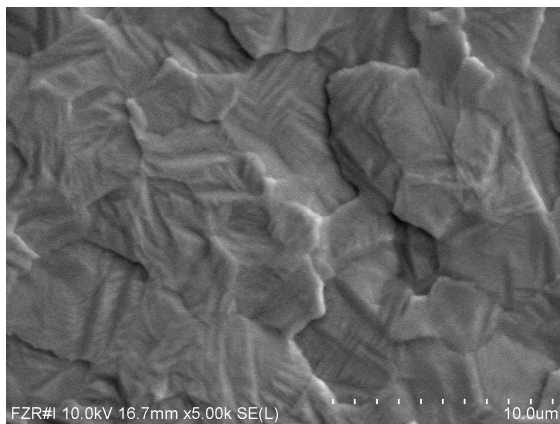


Fig. 4. SEM image of the irradiated surface

Appearance of these metastable phases results in high residual stress values in the irradiated target. In such a way the subsequent nitrogen diffusion in the irradiated specimens will take place in the fine-grain structure and in the field of intrinsic mechanical stresses.

C. AES investigation of nitrated sample

In Fig. 5 the depth distribution of nitrogen and carbon obtained by AES is shown. One can see that the depth of penetration of nitrogen into the specimen bulk for the pre-irradiated specimen is noticeably larger than that for the non-irradiated one (110 and 170 nm, respectively). Moreover, the overall quantity of nitrogen absorbed by the pre-irradiated specimen during nitriding is two times as much as in the non-irradiated one. It is interesting to note, that along with an increase in depth of penetration for nitrogen, a decrease of that for carbon takes place. The latter reduces from 60 nm for non-irradiated sample to 15 nm for the irradiated one. The overall quantity of carbon in the pre-irradiated samples is lowered by a factor equals to 1.2. So, pre-irradiation of the titanium alloy leads to cleaning the material surface from impurities and simultaneously stimulates its saturation with nitrogen.

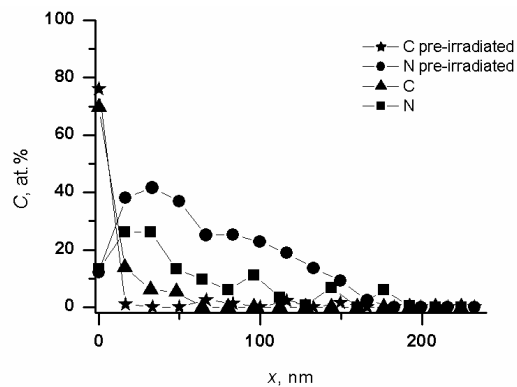


Fig. 5. AES element distribution profiles

D. XRD investigation of nitrated sample

From XRD data it follows that in the original state the Ti-6Al-4V alloy consists of two α and β phases. Approximate estimate gives that the fraction of the β phase in the non-processed sample is about 8 %.

After nitriding the phase composition of both pre-irradiated and non-irradiated titanium alloy samples has changed and the TiN and Ti_2N phases have appeared. The occurrence of these phases as a result of nitriding is predictable because it is well known that a modified zone after nitriding consists of three regions a layer of compound TiN followed by an Ti_2N layer and a diffusion layer underneath, which is an interstitial solution of nitrogen in the hcp α -titanium [1]. The formation of the TiN phase in the surface layer of the material is highly desirable due to

its appealing wear resistance properties. It should be noted however from the XRD data that the peaks of this phase are higher for pre-irradiated sample than those for non-irradiated one. It is known also that the height of a peak is proportional to the phase fraction. Consequently, it can be concluded from X-ray diffraction patterns that a fraction of these new appeared phases is much larger for the pre-irradiated before nitriding specimen than that for non-irradiated.

E. Discussion and conclusions

The data on XRD and AES are agreed with each other. Indeed the larger quantity of nitrogen absorbed when nitriding by the pre-irradiated sample leads to the higher fraction of TiN phase in its surface. The issue is in reasoning why the pre-irradiated sample is more prone to nitriding than the non-irradiated one. There are two major causes in favour of that.

The first one is a refinement of grains as a result of electron-beam melting and consequent fast cooling. It is well known that diffusion along the grain boundaries is carrying out more efficiently than that in the body of grains due to existence of a large number of various defects which reduce the activation energy for diffusion. Grain refinement when irradiating leads to the increasing of grain boundaries extension and results in enhancement of nitrogen diffusion.

Another important reason for enhancement of nitrogen diffusion in the surface layer is the appearance of residual stresses in the surface layers of the irradiated targets. It is well known and described elsewhere [7] that residual stresses occurring in the surface layer are the tensile stresses and from one hand they are deleterious because could course a

cracking of the surface but from the other hand these stresses favour the interstitial diffusion of atoms.

Thus, the combined treatment, involving pulsed e-beam pre-irradiation, subsequent cleaning and nitriding is promising and leads to increase in the absorption of nitrogen, the fractions of TiN and Ti₂N phases and the surface microhardness in processed titanium alloy.

Acknowledgements

Authors would like to thank Mr. K. Karlik for the assistance in irradiation of samples.

References

- [1] A. Zhecheva, W. Sha, S. Malinov, and A. Long, *Surf and Coat. Technol.* 200, 2192 (2005).
- [2] E.I. Meletis, *Surf and Coat. Technol.* 149, 95 (2002).
- [3] V.P. Rotshtein, R. Guenzel, A.B. Markov, D.I. Proskurovsky, M.T. Pham, et al., *Rus. Fizika i khimiya obrabotki materialov* 1, 62 (2006).
- [4] G.E. Ozur, D.I. Proskurovsky, V.P. Rotshtein, and A.B. Markov, *Laser and Particle Beams* 21, 157 (2003).
- [5] Yu.Kh. Akhmadeev, I.M. Goncharenko, Yu.F. Ivanov, N.N. Koval, P.M. Shcanin, *Rus. Pis'ma v ZhTF* 31, 24 (2005).
- [6] A.B. Markov, V.P. Rotshtein, *Nuclear Instruments and Methods in Physics Research B* 132, 79 (1997).
- [7] D.I. Proskurovsky, V.P. Rotshtein, G.E. Ozur, Yu.F. Ivanov, A.B. Markov, *Surf. and Coat. Technol.* 125, 49 (2000).